Enthalpy as Internal Energy in Plug Flow Reactor Models: a Long-Lasting Assumption Defeated and its Effects on Models Predictions in Dynamic Regime

Francesco Rossi[a,b], Eva M. Speelmanns[c], Tilman Barz[d], Carlo Pirola[e], Guenter Wozny[c], Flavio Manenti*[a,c]

[a] Politecnico di Milano, Dipartimento Chimica Materiali e Ingegneria Chimica "Giulio Natta", Piazza Leonardo da Vinci 32, 20133 Milano, Italy
[b] Purdue University, School of Chemical Engineering, Forney Hall of Chemical Engineering, 480 Stadium Mall Drive, West Lafayette, IN 47907-2100, USA
[c] Technische Universität Berlin, School of Process Sciences, Department of Process Dynamics and Operation, Sekr. KWT-9, Straße des 17. Juni 135, D-10623 Berlin, Germany
[d] Austrian Institute of Technology AIT, Energy Department, Giefinggasse 2, 1210 Wien, Austria
[e] Università degli Studi di Milano, Dipartimento di Chimica, via Golgi 19, 20133 Milano, Italy
flavio.manenti@polimi.it

In this paper, a general dynamic model of a pseudo-homogeneous catalytic plug flow reactor (PFR) is developed, which does not apply the traditional assumption of negligible difference between enthalpy and internal energy inside its energy balance. Such a model is then compared to a second dynamic PFR model, whose energy conservation equation identifies internal energy with enthalpy. The aim is that of quantitatively investigating the real suitability of the identification of these two thermodynamic quantities (internal energy and enthalpy) in PFR modeling problems. The Claus process is selected as a meaningful case study for the aforementioned purposes.

1. Introduction

Nowadays, heterogeneous catalysis rules in almost all industrial processes, especially in the form of heterogeneous gas-solid plug flow reactors (PFRs). These process units have been deeply investigated in chemical engineering history and several first-principles modeling strategies have been developed to predict both their steady-state and their transient operation. Such models can be very useful for several different purposes, such as: (I) the process dynamic simulation/optimal design towards a better phenomenological understanding/operation of the process itself; (II) the steady-state/dynamic optimization towards improved process economics; (III) the model-based optimal control to ensure fast and safe rejection of external perturbations and production grade switches; etc.. Most of these applications have already been widely broached in the literature. For instance, the energy intensification of a fixed-bed methanol reactor is addressed in (Manenti et al., 2013) while the 2D dynamic modeling of a fixed-bed Fisher-Tropsch reactor is studied in (Pratt, 2011). Moreover, a systematic optimal design strategy for PFRs is described in (Hillestad, 2010) and the catalyst optimization for a reactor of the same type is performed in (Pirola et al., 2009). The dynamic optimization and optimal control of PFRs are much more challenging due to the numerical complexity of the resulting problem. However, several authors have successfully tested themselves with them. For example, Manenti and Bozzano (2013) provides a strategy for the optimal control of fixed-bed methanol reactors and Shahrokhi and Baghmisheh (2005) studies the modeling, simulation and control of the same units. In addition, the work of Zavala and Biegler (2009a) deals with an optimal control framework for low-density polyethylene tubular reactors and the same authors propose some advances to the standard model predictive control algorithms for the same types of unit (Zavala and Biegler, 2009b). Finally, the dynamic optimization of a low-

density polyethylene plant, including a flow reactor, is faced and solved by Cervantes et al. (2002). It is undeniable that all the aforementioned applications, which rely on PFR models, require elevated accuracy and reliability of the model predictions. One assumption that is often introduced when a PFR is modeled is that of neglecting the difference between internal energy and enthalpy in the energy balance, regardless the instructions included in several well-known textbooks as (Bird et al., 2007). Indeed, it is assumed that, at least at low pressures, the resulting error in the model predictions is not relevant. However, there is lack of quantitative information concerning the suitability of this simplifying assumption. The aim of this paper is to try to fill this emptiness. Therefore, in this article, a detailed general dynamic pseudo-homogeneous model of a catalytic PFR is developed, which explicitly accounts for the difference between internal energy and enthalpy in the energy balance. Then, also a conventional version of PFR model is built and some simplifications are identified as to neglect the pressure dependence in the energy conservation equation. Finally, the two models are used to simulate the first catalytic layer of an existing Claus process catalytic reactor and the achieved results are compared in both steady-state and transient regime. This comparison should quantitatively demonstrate whether the assumption of negligible difference between enthalpy and internal energy is feasible in PFR models, without compromising the accuracy and reliability of their predictions, especially at low pressures.

2. Pseudo-homogeneous detailed and conventional PFR dynamic model

This section addresses the modeling of a generic PFR (Figure 1), with both detailed and conventional strategies. The detailed model is the first to be discussed but, before doing this, the employed simplifying assumptions must be introduced.

The simplifying assumptions on the gas phase include: (I) perfect gas behavior; (II) temperature-independent thermodynamic properties (constant pressure and constant volume specific heat, enthalpy of reaction and so on); (III) temperature-independent and composition-independent transport properties (axial dispersion and thermal conductivity, viscosity, global heat transfer coefficient and so on); (IV) no gas phase-catalytic phase gradients. The assumptions on the catalytic phase consist of: (I) isothermal catalyst particles; (II) no diffusive limitations inside the catalyst (the efficiency factor equals one). Finally, an additional assumption relates to the reactor refrigerating system. Indeed, the coolant is supposed to be a phase changing fluid, thus its temperature is considered constant.
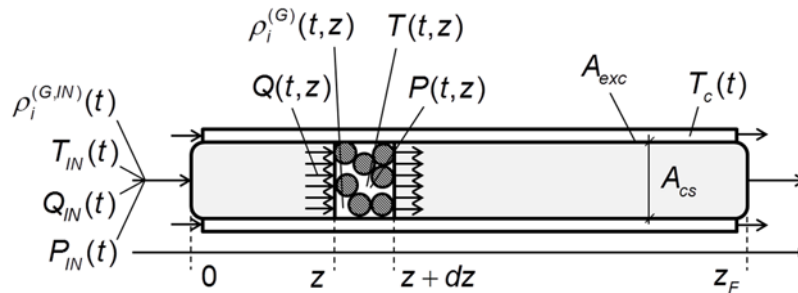

Figure 1: Generic PFR schematic drawing

Starting now with the detailed description of the PFR model, the necessary equations include: the component material balances (Eq(1)), the energy balance (Eq(2)) and two additional expressions to predict the pressure losses (Eq(3)) and the volumetric flow variation (Eq(4)).

$$\frac{\partial \rho_i^{(G)}}{\partial t} = -\frac{1}{\varepsilon A_{cs}} \frac{\partial}{\partial z}\left(\rho_i^{(G)} Q\right) + D_i^{eff} \frac{\partial^2 \rho_i^{(G)}}{\partial z^2} + \frac{1-\varepsilon}{\varepsilon} PM_i \sum_{j=1}^{N_R} v_{ij} R_j^{(r)} \tag{1}$$

Several symbols included in Eq(1) have to be explained. In detail, $\rho_i^{(G)}$ stands for mass concentration of the i-th component inside the reactor, ε represents the catalytic bed void fraction, A_{cs} stands for reactor vessel cross-sectional area, Q is the volumetric flowrate inside the reactor, D_i^{eff} is the effective axial dispersion of the i-th component, PM_i identifies the molecular mass of the i-th component, N_R is the number of chemical reactions, v_{ij} represents the stoichiometric coefficient of the i-th component in the j-th reaction and $R_j^{(r)}$ is the rate of the j-th reaction.

$$\frac{\partial T}{\partial t} = \frac{1}{\varepsilon \sum\limits_{i=1}^{N_C} \rho_i^{(G)} Cv_i + (1-\varepsilon)\rho_c Cp_c} \begin{bmatrix} -\frac{Q}{A_{cs}} \sum\limits_{i=1}^{N_C} \rho_i^{(G)} Cp_i \frac{\partial T}{\partial z} - (1-\varepsilon) \sum\limits_{j=1}^{N_R} \Delta H_{R_j} R_j^{(r)} + k^{eff} \frac{\partial^2 T}{\partial z^2} + \\ +\frac{U}{A_{cs}} \frac{dA_{exc}}{dz} (T_c - T) - \frac{P}{A_{cs}} \sum\limits_{i=1}^{N_C} \frac{1}{\rho_i^{(P)}} \frac{\partial}{\partial z} (\rho_i^{(G)} Q) + \\ +P(1-\varepsilon) \sum\limits_{i=1}^{N_C} \frac{PM_i}{\rho_i^{(P)}} \sum\limits_{j=1}^{N_R} v_{ij} R_j^{(r)} \end{bmatrix} \quad (2)$$

Also Eq(2) contains some acronyms not yet defined. In detail, T is the temperature inside the reactor, N_C identifies the number of components in the reacting mixture, Cv_i stands for i-th component constant volume specific heat inside the reactor, ρ_c is the catalyst intrinsic density, Cp_c stands for catalyst constant pressure specific heat, Cp_i stands for i-th component constant pressure specific heat inside the reactor, ΔH_{R_j} is the enthalpy of reaction for the j-th reaction, k^{eff} is the effective axial thermal conductivity, U is the global heat transfer coefficient, A_{exc} stands for reactor vessel thermal exchange area, T_c represents the coolant temperature, P stands for pressure inside the reactor and $\rho_i^{(P)}$ is the density of the i-th pure component. A couple of additional remarks on Eq(2) must be added. First, the reader should notice the presence of two unusual terms in the energy balance, whose formulation explicitly includes the reactor pressure. These are the terms taking into account the difference between enthalpy and internal energy. Second, it is important to briefly report how one can derive the mathematical expression in Eq(2). The idea is to write a rigorous energy balance, replace internal energy with enthalpy based on its thermodynamic definition and, finally, use the species material balances (Eq(1)) to eliminate the mass-dependent time-related partial differential terms.

$$\frac{\partial P}{\partial z} = -\frac{1-\varepsilon}{\varepsilon^3} \frac{G}{DP_c \sum\limits_{i=1}^{N_C} \rho_i^{(G)}} \left[1.75G + 150(1-\varepsilon) \left(\frac{\mu_{mix}^{(G)}}{DP_c} \right) \right] \quad (3)$$

Additional symbols concerning Eq(3) must be discussed. In detail, G represents the mass flowrate per unit cross-sectional area inside the reactor, DP_c is the catalyst particles diameter and $\mu_{mix}^{(G)}$ is the reacting mixture viscosity. Notice that this formula is the well-known Ergun correlation for the evaluation of pressure drops in packed beds and is derived under the assumption of steady-state conditions (Ergun, 1952). However, here it is applied in transient conditions. This is a feasible assumption, since the momentum dynamics are much faster than the material and thermal dynamics and therefore no significant inaccuracies in the PFR model predictions are introduced.

$$Q = Q_{IN} \left(\frac{T}{T_{IN}} \right) \left(\frac{P_{IN}}{P} \right) \left(\frac{PM_{mix}^{IN}}{PM_{mix}} \right) \quad (4)$$

The last main equation of the detailed PFR model to be discussed is Eq(4). As for Eq(1-3) some new acronyms need to be explained: Q_{IN} stands for inlet volumetric flowrate, T_{IN} indicates the temperature of the reactor feed, P_{IN} is the pressure of the reactor feed, PM_{mix} is the molecular mass of the reacting mixture inside the reactor and PM_{mix}^{IN} identifies the molecular mass of the inlet mixture. Eq(4) is derived from the perfect gases equation of state and is used to replace the mono-dimensional Navier-Stokes equation. In other words, a rigorous modeling strategy would include the Navier-Stokes equation plus an equation of state while here the Ergun equation and an equation of state are employed. This approach is a smart strategy to significantly simplify the numerical complexity of the resulting PFR model without introducing critical errors on its predictions.

Up to now, the main equations constituting the PFR detailed model have been analyzed. However, a formula to compute the reaction rates has to be chosen. This formula is selected as a generalized Langmuir-Hinshelwood rate equation because this choice provides the model with a high degree of generality. The mathematical structure of this generalized rate equation is not reported both for the sake of brevity and because it is not essential to the aims of the work. Moreover, since Eq(1-3) are PDEs (partial differential

equations) a proper set of initial and boundary conditions must be defined. First of all, Eq(1) and Eq(2) require an initial condition. This condition contains information on the zero-time operation of the PFR. Instead, Eq(3) is an exception and does not require any initial condition because no temporal derivatives can be found inside it. In addition, boundary conditions for Eq(1), Eq(2) and Eq(3) are required. However, for Eq(1-2) the standard Danckwerts conditions can be employed (zero-gradient at the end of the reactor and a set of material/energy balances at the reactor inlet interface). Instead, for Eq(3) only a condition at the reactor inlet is required, which can be chosen to impose the continuity of the pressure field. Once again, the detailed mathematical representation of these initial and boundary conditions is not reported for the sake of brevity but the interested reader can easily find them in previous literature papers.

At this point the detailed PFR model has been completely addressed and described. Now the conventional PFR model should be analyzed. However, the only differences between the standard and detailed model reside in the energy balance formulation. Therefore, the only equation of the conventional model that is explicitly reported here is the energy balance. Refer to the detailed model explanation for any other equation and initial/boundary condition along with for the simplifying assumptions.

The conventional PFR energy balance is reported in Eq(5).

$$\frac{\partial T}{\partial t} = \frac{1}{\varepsilon \sum_{i=1}^{N_C} \rho_i^{(G)} Cp_i + (1-\varepsilon)\rho_c Cp_c} \left[\begin{array}{l} -\dfrac{Q}{A_{cs}} \sum_{i=1}^{N_C} \rho_i^{(G)} Cp_i \dfrac{\partial T}{\partial z} - (1-\varepsilon)\sum_{j=1}^{N_R} \Delta H_{R_j} R_j^{(r)} + k^{eff} \dfrac{\partial^2 T}{\partial z^2} + \\ +\dfrac{U}{A_{cs}} \dfrac{dA_{exc}}{dz}(T_c - T) \end{array} \right] \tag{5}$$

No additional symbols have to be explained here. However, notice that the two explicitly pressure-pendent terms, observed in Eq(2), are now missing. Finally, the reacting mixture heat capacity is here evaluated with the constant pressure specific heat while it is computed with the constant volume specific heat in Eq(2).

Now that also the conventional PFR model has been described, some considerations on the solution strategy employed to solve the two reported models (detailed and conventional) can be conveyed. Since both of them can be classified as PDAE (partial differential algebraic equations) systems, at first the MOL (method of lines) is adopted to reduce each PDAE system to a corresponding DAE (differential algebraic equations) system. The spatial derivatives discretization is addressed based on the backward Euler formula, thus ensuring unconditional stability. Then, the obtained DAE systems are integrated by means of the numerical tools included in BzzMath library (Buzzi-Ferraris and Manenti, 2012), downloadable from (Buzzi-Ferraris, 2014). Notice that the MOL application reduces an original PDAE system into a structured DAE system with a much greater number of equations. Therefore, it is essential to both optimize the original PDAE formulation and take advantage of this resulting DAE structure in order to simultaneously minimize the numerical complexity of the problem to be solved, reduce the computational times and lower the number of possible infeasible side-solutions that can be introduced by the algebraic sub-portion. In the current case, the aforementioned PDAE system optimal configuration is that in Eq(1-5). This is why these equations are shown in that specific form.
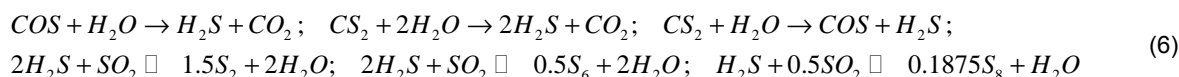
3. Case study: the Claus process catalytic reactor

The two PFR models (detailed and conventional), derived in the previous section, are now configured and employed to simulate the first catalytic layer of a Claus process catalytic reactor. At first, the aim is that of testing whether identifying enthalpy with internal energy in the energy balance of a PFR model is a feasible assumption, especially at low pressures. Secondly, the authors would like to quantify the error that is introduced by the aforementioned simplification.

Before entering into the details of the performed simulations and reporting the achieved results, let the simulated process unit be briefly described and the employed models configuration settings be explained.

Dealing with the simulated unit, the catalytic tabular reactor, whose first layer is used as reference system for this test case, is an equipment of an existing Claus process. In terms of layout, it is made of several adiabatic layers, approximately 0.5 m long, with intermediate cooling steps. The unit is used to convert H_2S and SO_2 to sulfur (S_x) and operates at approximately 250 – 300 °C and 1.5 atm. The employed catalytic phase is alumina. No other specific information can be added to avoid the disclosure of restricted data.

Coming to the employed models configuration, a simplified kinetic scheme for the simulated process (Eq(6)) is selected and inserted into the two PFR models (detailed and conventional). In addition, the proper initial and boundary conditions are applied and the physical/transport properties of the reacting mixture, along with the first reactor layer structural data, are implemented into the models (heat transfer coefficients are set to zero since the simulated system is adiabatic).

$$COS + H_2O \rightarrow H_2S + CO_2; \quad CS_2 + 2H_2O \rightarrow 2H_2S + CO_2; \quad CS_2 + H_2O \rightarrow COS + H_2S;$$
$$2H_2S + SO_2 \ \square \ 1.5S_2 + 2H_2O; \quad 2H_2S + SO_2 \ \square \ 0.5S_6 + 2H_2O; \quad H_2S + 0.5SO_2 \ \square \ 0.1875S_8 + H_2O \tag{6}$$

After correctly configuring the detailed and conventional PFR models, several simulations are carried out. At first, three steady-state simulations are performed, one at the nominal operating pressure (~1.5 atm) and two at higher pressures, i.e. twice and three times the standard working pressure. The achieved results, including the PFR axial temperature profiles along with some key components axial trends, are shown in Figure 2.
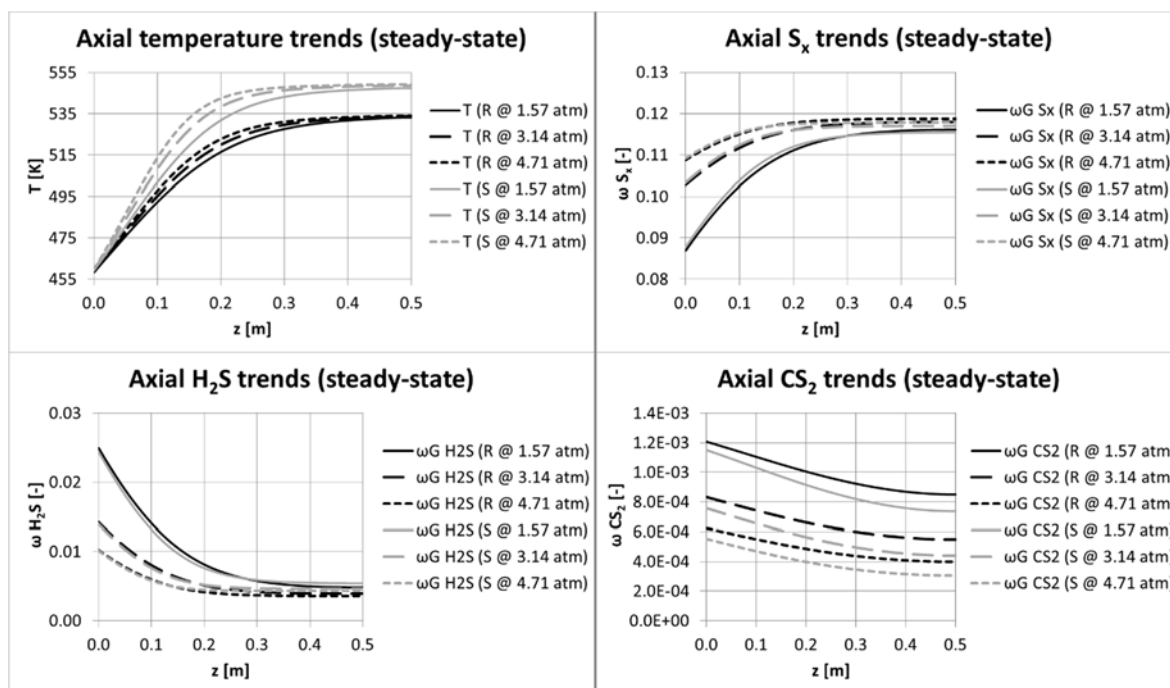

Figure 2: Steady-state simulations at different pressures (R and S stand for the results of the detailed and conventional models, ω stands for mass fraction and S_x for all the produced sulfur)

Notice that the difference among the predictions of the detailed and conventional PFR model is relevant, even at low pressure (~1.5 atm). For instance, at 1.57 atm, the conventional model overestimates the reactor temperature by about 15 °C while underestimates the production of CS_2, which is a very powerful catalysts poison, by about 5 %. Moreover, as the PFR operating pressure increases, the difference in the predictions of the two models increases but not so relevantly. Therefore, the data reported in Figure 2 are quite in contrast with the nowadays well-established modeling beliefs on tabular reactors and, in the opinion of the authors, introduce relevant novelties in the plug flow reactors modeling area.
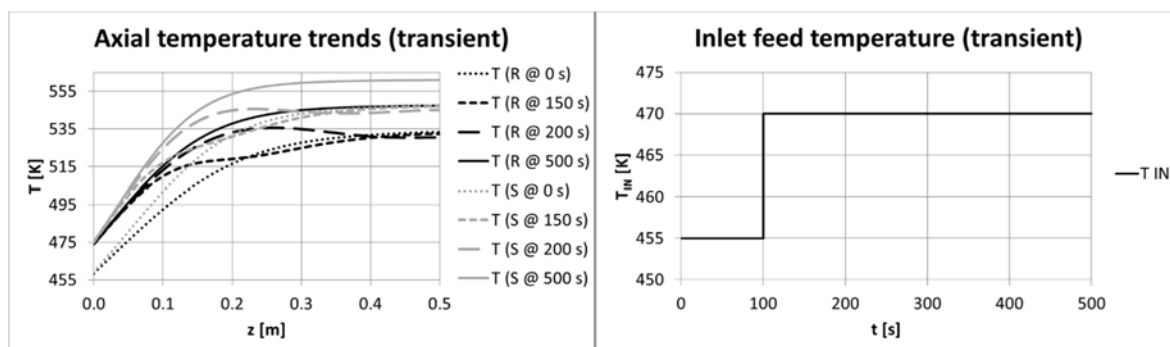

Figure 3: Dynamic simulation at 1.57 atm (R and S stand for the results coming from the detailed and conventional models)

After the steady-state simulations, an additional simulation is performed in dynamic regime to investigate the difference in the predictions of conventional and detailed PFR models also in this circumstance. The results are shown in Figure 3.

Also in this case, some differences between the results coming from the detailed and the conventional PFR model can be found. In detail, the dynamics predicted by the detailed model is a bit slower than that foreseen by the conventional model. Moreover, the shape of the dynamic profiles is slightly different.

As a final remark, observe that Figure 2 and Figure 3 jointly suggest that using a conventional PFR model might result in some general and unwanted effects: (I) overestimation of tabular reactors hotspots; (II) over/underestimation of key compounds conversions/production; (III) slight overestimation of the characteristic dynamic times. All these effects might take to economic losses due to excessive caution in reactors optimization, need for unpredicted catalyst beds replacement for poisoning effects, etc. Moreover, the aforementioned inaccuracy problems might also take to safety risks when model-based control systems and/or online optimization suites are applied to real industrial units. In the end, the difference between internal energy and enthalpy in the energy balance of PFR models should never be neglected, even at low pressure.

4. Conclusions

In this paper, a detailed PFR model is developed that does not rely on the typical assumption of negligible difference between internal energy and enthalpy in the energy balance. The predictions guaranteed by this model are compared to those ensured by a conventional alternative, in both steady-state and dynamic regime. Simulations at low to medium pressures are performed. The achieved results demonstrate that the conventional assumption of identifying enthalpy with internal energy in the flow reactors energy balance leads to relevant inaccuracies, even at low pressures. This is a quantitative proof that defeats this well-established and wide-spread thumb rule and suggests the systematic application of the detailed PFR modeling strategy.

References

Bird R. B., Stewart W. E., Lightfoot E. N., 2007, Transport phenomena, John Wiley & Sons.

Buzzi-Ferraris G., 2014, BzzMath library for scientific computing <www.chem.polimi.it/homes/gbuzzi> accessed 25.11.2014.

Buzzi-Ferraris G., Manenti F., 2012, BzzMath: Library Overview and Recent Advances in Numerical Methods, Computer Aided Chemical Engineering, 30(2), 1312-1316.

Cervantes A. M., Tonelli S., Brandolin A., Bandoni J. A., Biegler L. T., 2002, Large-scale dynamic optimization for grade transitions in a low density polyethylene plant, Computers and Chemical Engineering, 26, 227–237.

Ergun S., 1952, Fluid flow through packed columns, Chemical Engineering Progress, 48, 89-94.

Hillestad M., 2010, Systematic staging in chemical reactor design, Chemical Engineering Science, 65(10), 3301-3312.

Manenti F., Leon-Garzon A. R., Bozzano G., 2013, Energy-Process Integration of the Gas Cooled/WaterCooled Fixed-Bed Reactor Network for Methanol Synthesis, Chemical Engineering Transactions, 35, 1243-1248.

Manenti F., Bozzano G., 2013, Optimal control of methanol synthesis fixed-bed reactor, Industrial and Engineering Chemistry Research, 52(36), 13079-13091.

Pirola C., Bianchi C. L., Di Michele A., Diodati P., Vitali S., Ragaini V., 2009, High loading Fe-supported Fischer-Tropsch catalysts: optimization of the catalyst performance, Catalysis Letters, 131(1-2), 294-304.

Pratt J. W., 2011, Development of a comprehensive and flexible model for fixed-bed Fisher-tropsch reactors, 2011 AIChE Annual Meeting, 1p.

Shahrokhi M., Baghmisheh G. R., 2005, Modeling, simulation and control of a methanol synthesis fixed-bed reactor, Chemical Engineering Science, 60, 4275 – 4286.

Zavala V. M., Biegler L. T., 2009a, Optimization-based strategies for the operation of low-density polyethylene tubular reactors: nonlinear model predictive control, Computers and Chemical Engineering, 33, 1735–1746.

Zavala V. M., Biegler L. T., 2009b, Optimization-based strategies for the operation of low-density polyethylene tubular reactors: Moving horizon estimation, Computers and Chemical Engineering, 33, 379–390.